

Neutron Cross-Section Measurements of ^{12}C between 14 and 25 MeV \dagger

F. BORELI, B. B. KINSEY, AND P. N. SHRIVASTAVA

The University of Texas, Austin, Texas 78712

(Received 15 January 1968)

Measurements of the elastic and nonelastic cross sections for neutrons on ^{12}C have been made over the energy range between 14 and 25 MeV using a spherical shell of scattering material surrounding a stilbene detector. In addition to the known peak in the elastic scattering at 19.5-MeV neutron energy, another has been found at 15.8 MeV. The widths of these peaks at half-maximum are 2.0 and 0.5 MeV, respectively. No resonance structure in the nonelastic scattering cross section was found. With specially designed scatterers, the differential elastic scattering was measured at angles which correspond to the zeros of the first four Legendre polynomials, viz., at 90° , 54.8° , 39.2° , and 30.5° . The excitation function of elastic scattering at these angles showed a similar resonance structure in each case, the weakest being at 90° . Inelastic neutron scattering to the first excited state of ^{12}C was determined between 14 and 21 MeV by measuring the 4.43-MeV γ rays produced by the decay of this state. A very small peak was found at 15.8 MeV and a broader rise near 19 MeV. The low level of resonant effects in the nonelastic channels suggests that the resonances observed in the elastic cross section are caused by single-particle states, and the differential measurements indicate that they are caused by p waves.

I. INTRODUCTION

THE existence of resonances at a high degree of excitation in ^{13}N has been established by studies of the elastic scattering of protons between 15 and 30 MeV. The angular distributions of elastic scattering show distortions ascribable to resonances for protons with energies near 22.5¹ and 26 MeV.² These proton energies correspond to excitation energies of 22.7 and 25.9 MeV, respectively. An analysis of the elastic scattering of protons between 20- and 30-MeV kinetic energy has been made by Tamura and Terasawa.³ These authors found that the observed scattering cross sections could be accounted for only on the assumption that the 22.5-MeV resonance is caused by a doublet, and that three resonances exist with the parameters shown in Table I. In other analysis of the same data, taking account of the published polarization data, Lowe and Watson⁴ also found that three resonances were required to give an adequate fit to the experimental data. Their findings are also shown in Table I. Both analyses were made by superposing resonance amplitudes on slowly varying or constant parameters of the optical model. Scott *et al.*⁵ have tried to account for the elastic scattering data and their own data on the inelastic scattering of protons leading to the 15.1-MeV state in ^{12}C by the assumption of intermediate (doorway) states. Their results are also shown in Table I. It will be seen that there is little agreement. The effect of resonances below 20 MeV was not taken into account in any of these calculations. However, the existence of such resonances is clear from the data of Daehnick and Sherr.⁶ Proton reaction cross sections have been studied by Makino

and Waddell,⁷ who found some evidence of resonance structure.

A level structure similar to ^{13}N should exist in the nucleus ^{13}C . An anomaly in the elastic scattering of neutrons, analogous to the proton resonance at 22.5 MeV, was first observed by Harlow *et al.*,⁸ the neutron energy being 19.5 MeV. The state corresponding to the higher-energy resonance in ^{13}N has not yet been observed in ^{13}C . Resonances in the total neutron cross section in this region are difficult to detect, although in the measurements of Harlow *et al.* there is some evidence of it. Some evidence for a resonance at neutron energy of 16 MeV was found by Cook and Bonner.⁹ There are additional isolated measurements of both total and non-elastic cross sections in this region, and also differential elastic scattering cross sections, the most accurate being in the vicinity of 14-MeV neutron energy.¹⁰⁻¹³ The present investigation was undertaken in order to see if the resonance anomaly seen in the elastic process is visible in inelastic channels.

II. EXPERIMENTAL ARRANGEMENT

Apparatus

The fast neutrons in the present measurements were obtained by bombarding a titanium tritide target with deuterons from the 4-MeV Van de Graaff accelerator of The University of Texas for the range 14 to 21 MeV, and from the tandem accelerator in the energy range above 21 MeV. The tritide target was mounted on a gold foil attached to the end of a brass tube with indium solder,

\dagger Supported in part by the U. S. Atomic Energy Commission.

¹ B. B. Kinsey, Phys. Rev. **99**, 332 (1955).

² J. Dickens, D. Haner, and C. Waddell, Phys. Rev. **132**, 2159 (1963).

³ T. Tamura and T. Terasawa, Phys. Letters **8**, 41 (1964).

⁴ J. Lowe and D. Watson, Phys. Letters **23**, 261 (1966).

⁵ D. Scott, P. Fisher, and N. Chant, Nucl. Phys. (to be published).

⁶ W. Daehnick and R. Sherr, Phys. Rev. **133**, B934 (1964).

⁷ M. Makino and C. Waddell, Nucl. Phys. **68**, 378 (1965).

⁸ M. Harlow, R. Robinson, and B. Kinsey, Nucl. Phys. **67**, 249 (1965).

⁹ C. F. Cook and T. W. Bonner, Phys. Rev. **94**, 651 (1954).

¹⁰ R. Clarke and W. Cross, Nucl. Phys. **53**, 177 (1964).

¹¹ M. Nakada, J. Anderson, C. Gardner, and C. Wong, Phys. Rev. **110**, 1439 (1958).

¹² J. Coon, R. Davis, H. Felthaus, and D. Nicodamus, Phys. Rev. **111**, 250 (1958).

¹³ J. Singletary and D. Wood, Phys. Rev. **114**, 1595 (1959).

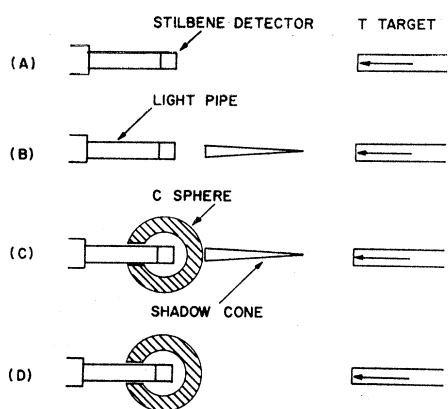


FIG. 1. Geometry for the total elastic and nonelastic scattering cross-section measurements.

and rotated. It was cooled by a water spray driven by compressed air.

It was found that reproducibility in neutron measurements depends as much on the stability and alignment of the beam as on the stability of associated electronic equipment. An exact alignment of detector and target and the shadow cone used in shielding the former from the latter was therefore necessary. For this purpose the area of the tritide target to be exposed to the beam was limited by a circular hole $\frac{1}{4}$ in. in diameter, cut in a tantalum plate placed some 12 in. in front of the rotating target holder. A quartz plate with a slightly larger hole in it, placed in front of this and viewed with the aid of closed circuit television allowed the focus and position of the beam to be adjusted so that all of it passed through the hole. A target holder, identical to that used for holding the tritide target and fitted with a quartz plate at its end protected by wire gauze, enabled the experimenter to determine the exact center to which the axis of the detector and shadow cone had to be aligned. The shadow cone was made from a machinable tungsten alloy, and supported by thin rods from an aluminum arm which could be rotated about a vertical axis passing through the tritide target. Varying the angle of emission of the neutrons relative to the deuteron beam allowed measurements to be made at different neutron energies without disturbing the beam in any way. If, then, the adjustment was properly made, the detector, a cylinder of stilbene 1 in. in length and 1 in. in diameter, was shielded from the neutron source at all angles by at least 10 in. of the shadow cone.

The detector which was mounted 24 in. from the source was viewed through a 6-in. light guide by a RCA 6810A photomultiplier connected to a neutron- γ -ray discriminating circuit. The pulses corresponding to neutrons from these circuits were fed into a PDP-7 computer and the spectrum of recoil protons in the stilbene detector plotted by a line printer.

In addition to this detector, another was mounted 24 in. from the neutron source, at 45° to the direction of the deuteron beam. This served as a monitor; all counts in its recoil spectrum having a pulse size above about half the maximum were recorded by a scaler.

Elastic and Nonelastic Scattering Measurements

For these measurements the scatterer consisted of a spherical shell of pure graphite of 6-in. o.d. and 3-in. i.d. A 1-in. hole drilled through it at the end allowed the stilbene detector to be placed at its center.

For each neutron energy, measurements were made with the four geometrical arrangements shown in Fig. 1. The typical recoil spectra obtained under these conditions are shown as A, B, C, and D, respectively, in Fig. 2. Taking the midpoint of the slope at the end of the spectrum (e.g., the point M in Fig. 2) as representative of the energy of the neutrons responsible for the proton recoil spectrum, a calibration curve of neutron energy against channel number was plotted. The neutron energy was varied by changing the angle of neutron emission relative to the deuteron beam. With the aid of this calibration, a point on the recoil spectrum could be chosen, 4 MeV below the neutron energy, such that all points on the recoil spectrum to the right of it are caused only by elastically scattered neutrons. Neutrons which leave ^{12}C in its 4.43-MeV state produce proton recoils to the left of this fiducial point. Only proton recoils to the right were recorded. That this procedure effectively excludes recoils caused by inelastically scattered neutrons may be seen from the curve (D) in Fig. 2, where the contribution of the group of neutrons leaving ^{12}C in its first excited state (4.43 MeV) is clearly seen.

The proton recoil spectra obtained in the four geometrical arrangements shown in Fig. 1 allow the following determinations of the number of neutrons reaching the detector: (A) without shadow cone or scatterer, (B) with the shadow cone shielding the detector, (C) with the scatterer surrounding the shielded

TABLE I. Comparison of theoretical analyses.

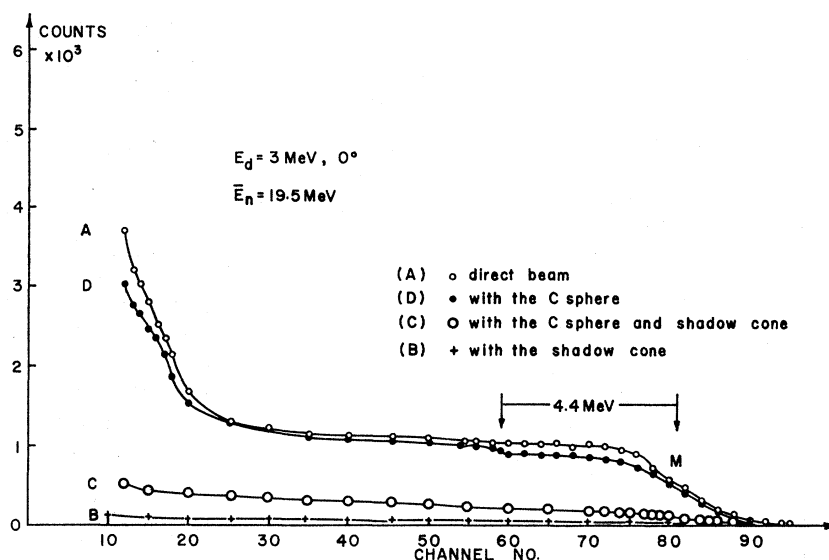
Tamura and Terasava ^a			Lowe and Watson ^b			Scott, Fisher, and Chant ^c	
Level	Excitation energy (MeV)	Width (MeV)	Level	Excitation energy (MeV)	Width (MeV)	Level	Excitation energy (MeV)
$d_{3/2}$	21.69	2.49	$g_{9/2}$	20.94	1.5	$d_{3/2}$	20.5
$d_{5/2}$	21.99	1.46	$h_{9/2}$	22.74	1.0	$f_{5/2}$	22.4
$p_{3/2}$	26.87	2.17	$f_{7/2}$	24.14	0.5	$p_{3/2}$	25.5

^a Reference 3.

^b Reference 4.

^c Reference 5.

FIG. 2. Sample of proton recoil spectra obtained with the stilbene detector; $E_d = 3$ MeV and $\theta = 0^\circ$. Four spectra A, B, C, and D correspond to the four geometrical arrangements (A), (B), (C), and (D) shown in Fig. 1.



detector, and (D) with the scatterer in position without the shadow cone. All these measurements were made for a given charge collected at the target (about 2000 μC), and only those proton recoils recorded which had energies above a point 4 MeV below the incident neutron energy. Usually about 20 000 counts were recorded above the selected fiducial point in condition A. Checks were made to ensure that both this counting rate and the shape of the recoil spectrum were independent of the beam current. The count B measures the background and was usually about 2% of A, when A was measured in the forward direction. (A-B) then, measures the undisturbed neutron flux, (C-B) measures the neutrons scattered elastically from the scatterer, and (A-D) measures the neutrons transmitted through the scatterer.

The quantity $(C-B)/(A-B)$, the fraction of the neutrons scattered, was usually determined to a statistical accuracy of about 3 to 5% in any individual measurement and $(A-D)/(A-B)$, the nonelastic scattering, to about 10%. Usually some three to five measurements were made at each angle, and the average taken. This procedure, if followed at one beam energy only, can give rise to uncertainties in the vicinity of 90° to the beam owing to the possibility of shadows of the neutron source being cast by the target holder or by the gold foil on which it was mounted. Although, in fact, no such shadows were observed, we thought it best to repeat measurements made at incident deuteron energies of 3.6 to 4 MeV, at 1.5 MeV. This procedure allowed the range 14- to 17-MeV neutron energy to be covered at angles less than those in which shadows might be cast. With deuteron beams up to 10 μA , no evidence was found to indicate either short- or long-term over-all deterioration of the tritide target. However, it was clear from the rotation of the target, that different parts of the target differed quite markedly

from others in neutron production. It is possible that this variation of yield is responsible for residual uncertainties in reproducibility (1 to 2%) not ascribable to statistical fluctuations.

4.43-MeV γ -Ray Measurements

It is well known that the cross section for inelastic scattering to the first excited state of ^{12}C accounts for half the total nonelastic cross section near 14 MeV. A measurement of this cross section as a function of energy through the resonance region is of obvious interest. This was done by measuring the yield of 4.43-MeV γ rays as a function of energy. Since most if not all the known $T=0$ states of ^{12}C above 4.4 MeV decay preferentially by production of α particles, the γ -ray production is a direct measure of the production of the first excited state by inelastic scattering. For neutron energies above 16 MeV, the $T=1$ states can contribute to the excitation of the 4.43-MeV state, but do so very feebly.¹⁴

The γ -ray measurements were made with a similar carbon scatterer and a 2×2 -in. NaI crystal. The geometrical arrangement and the sequence of measurements was the same as described above for the elastic scattering. Typical pulse-height distributions obtained with the carbon scatterer surrounding the crystal and shadow cone in front of it, as well as the background with the scatterer removed, are shown in Fig. 3; the difference shown by solid circles is the effect of the carbon scatterer.

In this measurement a complication arises because the process of bombardment of a tritide source impregnates the titanium layer with deuterium, which then becomes a source of neutrons from the $\text{D}(d,n)^3\text{He}$ reac-

¹⁴ J. Anderson, C. Gardner, J. McClure, M. Nakada, and C. Wong, Phys. Rev. 111, 572 (1958).

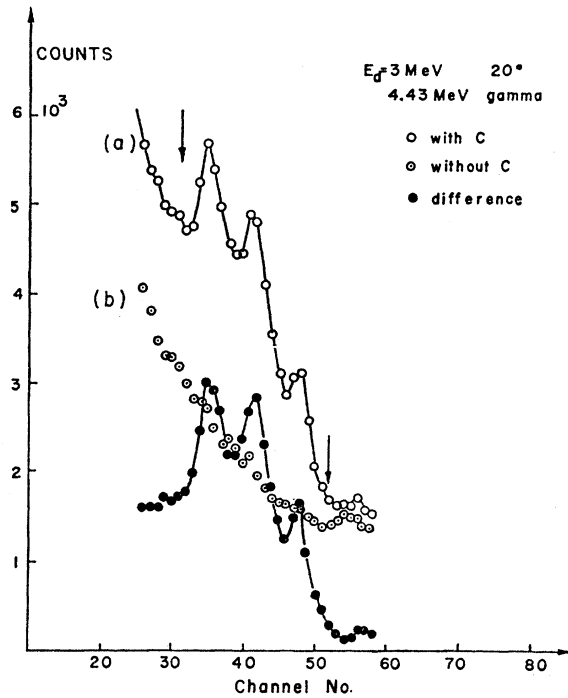


FIG. 3. A sample of the γ -ray spectra taken with the 2×2 -in. NaI(Tl) crystal detector; with the carbon scatterer in place (curve a) and with the scatterer removed (curve b). The curve with solid circles is the difference and represents the effect of the scatterer. The limits of the spectra from which the γ -ray yield was deduced are shown by the upper and lower arrow.

tion. The presence of these neutrons can be seen even in simple proton spectra of the type of Fig. 2. For the scattering measurements, with biased detection, the existence of these neutrons is of no consequence. However, for deuteron energies above 1.5 MeV, neutrons emitted in the forward direction from the $D(d,n)^3\text{He}$ reaction have sufficient energy to excite the 4.43-MeV state in ^{12}C by inelastic scattering (threshold 4.80 MeV). Consequently a correction must be made in the γ -ray measurements made with a tritide source for contributions caused by neutrons produced by deuterium. If Q is the measured γ -ray yield, the required corrected yield is $Q_c = Q - Q_d$, where Q_d is the yield due to neutrons produced by deuterium in the tritide target. To make this correction, the neutron fluxes from both tritium and deuterium targets were measured with the aid of a proton recoil neutron telescope, built in this laboratory according to a design of the CISE laboratory of Milan,¹⁵

¹⁵ G. Marazzan, M. A. Sona, and M. Pignarelli, *Nuovo Cimento* **10**, 155 (1958). The adjustment of this telescope spectrometer is of some interest. It was originally intended to adjust the voltages and the amplifications of the several proportional counters of which the spectrometer is made by passing α particles through a thin window at the front of the telescope; the polythene target, which is the source of recoil protons, being withdrawn on a wheel. However, it was found that this procedure was unnecessary, for the tritium target was itself a strong source of energetic protons with energies near 14 MeV. A study of these protons showed that they originate in the $^3\text{He}(d,p)^4\text{He}$ reaction; the ^3He , the product of tritium decay, being retained in the source. A source two

and the yield of γ rays from the deuterium target was obtained using the same geometry. Such corrections were about 10%.

Differential Elastic Scattering Measurements

Differential elastic scattering measurements were made at angles which would correspond to the emission of neutrons in the center-of-mass system at angles near the zeros of the first four Legendre polynomials (90° , 54.8° , 39.2° , and 30.5°). For this purpose special scatterers of carbon were machined in the form of cylinders of revolution, the sections through the axis being circular with radii chosen such that the circles pass through both the neutron source and the stilbene detector (Fig. 4). No attempt was made to measure the differential cross sections corresponding to the zeros of the Legendre polynomials in the backward direction, because, although the cross sections do not differ much from that at 90° , the necessary geometrical arrangement does not allow for counting rates much above the background. If the scatterer were infinitely thin and if the source and detector were points, the scattering angles at any point on the scatterer would be the same (a method used long ago by Amaldi *et al.*¹⁶). The thickness of the scatterers was such that scattering at the external and internal surfaces of the cylinders differed in angle by $\pm 4^\circ$, respectively, from the angle in the laboratory system corresponding to the zeros of the Legendre polynomials in the center-of-mass system. However, the detector (1×1 in.) was by no means a point, and the energy of the neutrons incident on the scatterer depends on the angle of neutron emission relative to the deuteron beam. The imperfections inherent in this arrangement were minimized by cutting off the end of the scatterer nearest to the detector in a plane perpendicular to the axis of the scatterer, and by two cuts

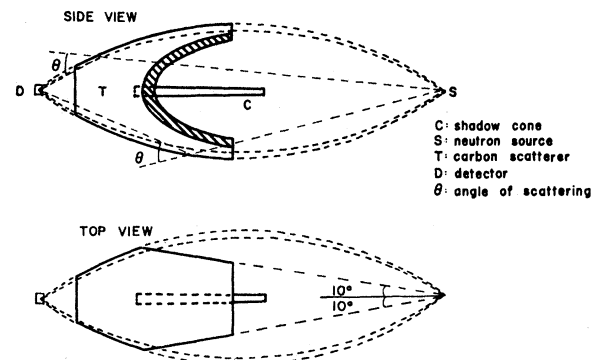
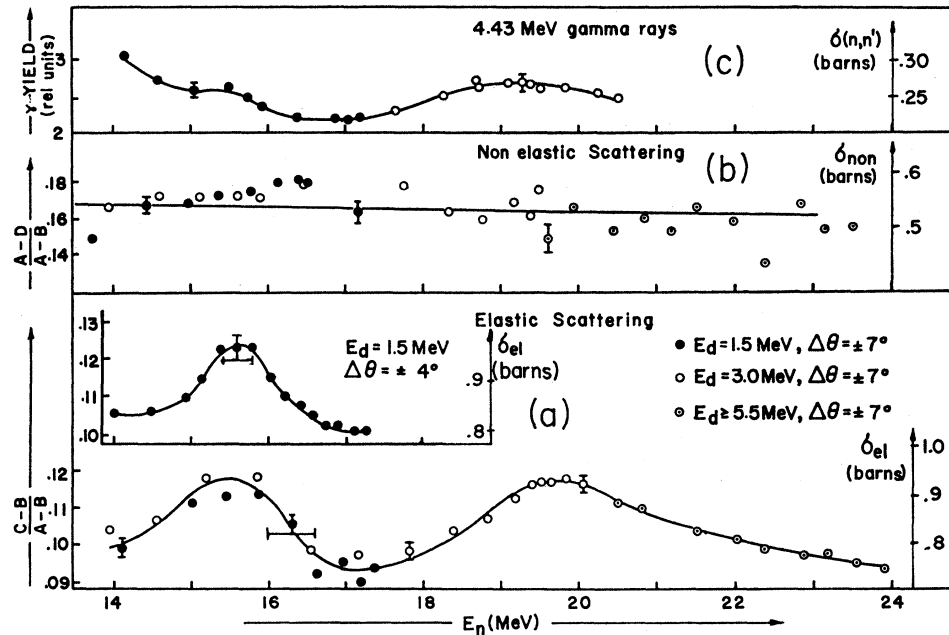


FIG. 4. Arrangement for the differential elastic scattering measurements: (a) Side view; (b) top view. The neutron source is at S; the detector at D; C is the shadow cone.

years old gives some 50 000 protons per second per unit solid angle in the forward direction with ample energy to penetrate the 0.010-in. gold backing on which the tritide is deposited.

¹⁶ E. Amaldi, D. Bocciarelli, B. Cacciapuoti, and G. Trabacchi, *Nuovo Cimento* **3**, 203 (1946).

FIG. 5. (a) Excitation curve for the total elastic scattering; the part of the curve near the lower-energy peak was repeated with a better energy resolution (insert); (b) nonelastic scattering; and (c) inelastic neutron scattering leading to the 4.43-MeV state in ^{12}C . $\Delta\theta$ is the angle subtended by the scattering sphere at the neutron source.



in a perpendicular plane such that the extremities of the scatterer do not subtend angles with the neutron beam differing by more than $\pm 10^\circ$ from the axis (see Fig. 4).

The geometrical arrangement is not conducive to making absolute measurements because the mean thickness of material between the detector and any point where a neutron is scattered is too great to make an approximate calculation worthwhile. Absolute cross sections were therefore obtained using the known absolute differential cross sections at 14 MeV.¹³

III. RESULTS

The total elastic scattering data are shown in Fig. 5(a) where the ratio $(C-B)/(A-B)$ is plotted against incident neutron energy. From this it is clear that the broad 19.5-MeV peak has a width of about 2 MeV. The experimentally determined width depends on the energy resolution of the incident neutron beam, which in its turn depends on the angle subtended by the sphere at the source and on the angle of emission of the neutrons. The measurements in the region of the 19.5-MeV peak were made mostly in the forward direction where the energy spread is much less than the observed width of the peak. However, for measurements near the 15.8-MeV peak, rather high angles of emission of the neutrons relative to the deuteron beam were required. A repetition of the measurements with an increased distance (44 in.) between source and detector [see insert in Fig. 5(a)] showed clearly that the width of this peak was dependent on the angle subtended by the scatterer at neutron source ($\Delta\theta$). The observed widths and the height of this peak relative to the continuum indicates that its true width is near 0.5 MeV.

The ratio of the counting rates, $(C-B)/(A-B)$, which determines the elastic scattering, is about 0.10 off resonance. That which determines the nonelastic scattering, $(A-D)/(A-B)$, is about 0.15. For an infinitely thin shell these ratios would give directly the product of the respective cross sections with the number of atoms per unit volume and the thickness of the shell. For a finite thickness however, as shown by Bethe *et al.*,¹⁷ the experimental ratios will be much lower. The elastic ratio $(C-B)/(A-B)$ should be

$$(1 - T_0)(\sigma_{et}/\sigma_t)e^{-\sigma_{tr}n \times L/2},$$

where $T_0 = \exp(-\sigma_t n X)$, σ_t is the total cross section, X is the difference in radii, n is the number of atoms per unit volume (0.88×10^{23} atoms per cm^3), σ_{tr} is the total transport cross section (viz., $\sigma_{tr} = \sigma_n + \sigma_{et}$, σ_n being the nonelastic and σ_{et} being the elastic transport cross section); and $L = \frac{3}{2} + \ln(2r_2/X)$, where r_2 is the external radius of the shell. At 14.2 MeV $\sigma_n = 0.6$ b and $\sigma_t = 1.4$ b^{13,18} and the elastic transport cross section $\sigma_{et} \approx 0.35$ b. These figures give a ratio of 0.12, compared to the observed value of 0.10. The difference lies in the fact that the efficiency of detection, neglecting the variation in energy of the neutron-proton cross section, falls linearly with the energy. Approximately, the energy of neutrons scattered at angle θ is $E(\theta) \approx E_0[1 - (2/A)(1 - \cos\theta)]$, where E_0 is the energy of the incident neutron and A is the mass number of the scatterer. The detection efficiency then is proportional to $[E(\theta) - (E_0 - \Delta)]/\Delta$, where Δ is the distance in energy units of the detector

¹⁷ H. Bethe, J. Beyster, and R. Carter, *J. Nucl. Energy* **3**, 207 (1956).

¹⁸ M. MacGregor, W. Ball, and R. Booth, *Phys. Rev.* **108**, 726 (1957).

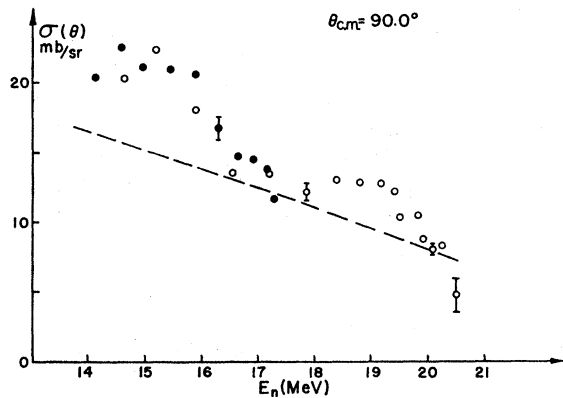


FIG. 6. Excitation curve for the differential elastic scattering at 90.0° (c.m.); the measurements were normalized at 14.2 MeV (Ref. 13). Solid and open circles correspond to measurements with deuterons of 1.5 and 3 MeV, respectively.

bias point below the neutron energy (E_0). The net effect is then proportional to

$$\int \left(\frac{d\sigma_{el}}{d\Omega} \right) \left[1 - (1 - \cos\theta) \frac{2E_0}{A\Delta} \right] d\Omega = \sigma_{el} \left[1 - (\sigma_{et}/\sigma_{el}) \frac{2E_0}{A\Delta} \right],$$

which means a reduction in efficiency by the factor

$$\left[1 - (\sigma_{et}/\sigma_{el}) (2E_0/A\Delta) \right],$$

provided that $\Delta > 4E_0/A$. If this condition does not hold, the range of integration is less than the whole range of $\cos\theta$. For $\Delta = 4$ MeV this factor is approximately 0.8, which, when taken together with the expression above, gives the ratio observed. It accounts also, approximately, for the observed variation of the ratio $(C-B)/(A-B)$ with Δ .

The results for the nonelastic measurements are shown in Fig. 5(b), where the ratio $(A-D)/(A-B)$ is plotted against incident neutron energy. There is no evidence here for any resonance effect above some 5% of the mean.

The nonelastic ratio¹⁷ is given by

$$(1 - T')\sigma_n / (\sigma_n + \sigma_{et}P),$$

where $T' = \exp(-\sigma_{tr}nX)$; P is the mean probability that a neutron once-scattered elastically in the scatterer will escape without suffering further inelastic collisions. P has been tabulated¹⁷; in the present experiment $P \approx 0.7$. This formula gives good agreement with the ratio observed.

The measured yield of 4.43-MeV γ rays is shown in relative units against the incident neutron energy in Fig. 5(c). Again there is no conclusive evidence for resonance effects. A rise in the yield near 19 MeV is probably not a resonant effect for it compensates a fall

in the $(n, n3\alpha)$ cross section¹⁹ and there is no evidence for it in the nonelastic cross section.

The results of the differential-cross-section measurements are shown in Figs. 6 to 9. The resonances show up clearly at each angle, although the net effect is much lower for 90° than for the other angles. Harlow *et al.*⁸ also measured the differential cross section at various angles in the energy range between 17.2 and 21.0 MeV, and found no evidence of resonance effect at 90° near 19 MeV.

IV. DISCUSSION

We consider first the nonelastic cross section. This, as we have seen, shows no resonance at either of the

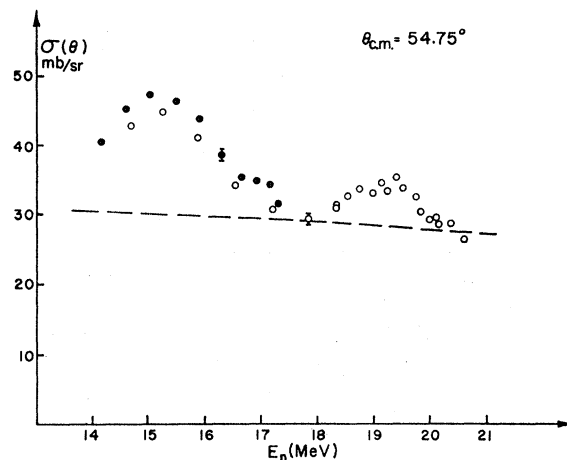


FIG. 7. Excitation curve for the differential elastic scattering at 54.75° (c.m.); the measurements were normalized at 14.2 MeV (Ref. 13). Solid and open circles correspond to measurements with deuterons of 1.5 and 3 MeV, respectively.

two resonances which appear in the elastic cross section. The ratio measured in the nonelastic measurements is less than that which would result from measurements made with an infinitely thin spherical shell. The reduction depends to some extent on elastic scattering through the elastic transport cross section. One might then expect a reduction in a possible resonant effect in the measured nonelastic ratio resulting from a resonance in the elastic cross section. A numerical estimate of this effect shows that it is small and certainly no larger than 5% of the total nonelastic cross section. We conclude therefore that the absence of a peak in the nonelastic cross section is real, and if there is such a peak, it must be less than 5% of the total, i.e., 30 mb or less.

The peak elastic cross section is $4\pi\lambda^2g\mu^2$ and the peak nonelastic cross section is $4\pi\lambda^2g(\mu - \mu^2)$, where μ is the ratio of the neutron width to the total width, λ is the wavelength in the center-of-mass system divided by 2π , and g is a statistical factor that has a value $l+1$ or

¹⁹ G. Frey, L. Rosen, and L. Stewart, Phys. Rev. **99**, 1375 (1955).

according as the spin of the resonant state is $j=l+\frac{1}{2}$ or $l-\frac{1}{2}$, l being the orbital angular momentum. These formulas and the absence of resonant effects in the non-elastic cross section put restrictions on the possible values of μ . The ratio of the peak nonelastic to the peak elastic cross sections is $(1/\mu-1)$. The peaks of the resonant elastic cross sections are above 0.18 b. Thus the ratio of peak nonelastic to elastic cross section is less than 0.2. This corresponds to $\mu > 0.8$, predominately elastic scattering, and a relatively large reduced neutron width compared to the Wigner limit.

We have attempted to analyze the results of the elastic scattering measurements by assuming that each resonance observed is the result of a single resonant state. This seems to be a reasonable assumption to make for the 15.8-MeV resonance, but it is very questionable for the 19-MeV resonance. We add a resonant amplitude to an optical potential scattering amplitude of the form $Ae^{i\delta_A} + Be^{i\delta_B}$, given by a computer program due to Perey,²⁰ the total potential elastic scattering cross section being $A^2 + B^2$. Both phases δ_A and δ_B tend to 90° as the angle of scattering tends to zero. The resonance amplitude at a scattering angle θ has components

$$a(\theta) = (i/2k)[(l+1)(1 - e^{2i\delta_{l^+}}) + l(1 - e^{2i\delta_{l^-}})]P_l(\cos\theta)$$

and

$$b(\theta) = (i/2k)[e^{2i\delta_{l^+}} - e^{2i\delta_{l^-}}]P_l'(\cos\theta),$$

where lh is the orbital angular momentum, $P_l(\cos\theta)$ is

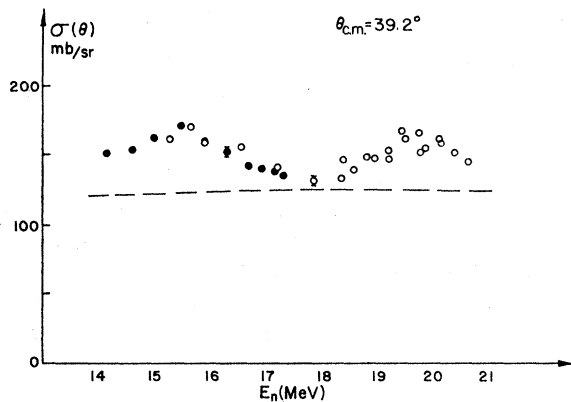


FIG. 8. Excitation curve for the differential elastic scattering at 39.2° (c.m.); the measurements were normalized at 14.2 MeV (Ref. 13). Solid and open sides correspond to measurements with deuterons of 1.5 and 3 MeV, respectively.

the Legendre polynomial of order l , and $P_l'(\cos\theta) = \sin\theta(d/d\cos\theta)P_l(\cos\theta)$. The phases δ_{l^+} and δ_{l^-} refer

²⁰ An optical-model program, version III S-S. The real part of the potential was $(49.3 \text{ MeV}) - 0.33E_n$ (where E_n is the incident neutron energy), of Saxon-Woods form, with a radius equal to $1.25A^{1/3} \text{ F}$, the diffuseness being given by the parameter $a=0.65 \text{ F}$; the imaginary part was a surface potential (the derivative of a Saxon-Woods potential), the depth being 5.75 MeV, but with a diffuseness given by $b=0.70 \text{ F}$, and a spin-orbit potential of the same general type with a depth of 5.5 MeV and a diffuseness of 0.65 F.

to the two partial waves with $j=l\pm\frac{1}{2}$. These phases are given by

$$1 - e^{2i\delta_l} = i\Gamma\mu/(E - E_0 + \frac{1}{2}i\Gamma),$$

where Γ is the total width and E_0 is the resonance energy.

Assuming that only one or the other of the two possible values of the total angular momentum j is of importance, one or the other of the resonance phases is equated to zero, and the total differential cross section for elastic scattering is

$$\begin{aligned} d\sigma^\pm/d\Omega &= [Ae^{i\delta_A} + a]^2 + [Be^{i\delta_B} + b]^2 \\ &= A^2 + B^2 + \mu^2\lambda^2[P_l'^2 + g_\pm^2 P_l^2] \sin^2\varphi \\ &\quad + 2A\lambda g_\pm P_l\mu \sin\varphi \cos(\varphi - \delta_A) \\ &\quad \mp 2B\lambda P_l'\mu \sin\varphi \cos(\varphi - \delta_B), \end{aligned} \quad (1)$$

where

$$\tan\varphi = \Gamma/2(E_0 - E),$$

$$g_+ = l+1 \text{ for } j=l+\frac{1}{2}, \text{ and } g_- = l \text{ for } j=l-\frac{1}{2}.$$

In this expression, both A and B , and the phases associated with them are functions of the scattering angle. The sum of the squares of their moduli gives a fairly good fit to the known differential elastic scattering cross section near 14 MeV. Since neither A nor B , nor the phases associated with them, change much over a small range of energy, it was sufficient to calculate the differential cross sections as a function of energy taking these quantities to be those calculated from Perey's program at 16 MeV. The width Γ is given directly by the experiments; we have assumed that Γ is 400 keV for the 15.8-MeV resonance. The only really adjustable parameter is μ . Taking $\mu=0.7$ for the 15.8-MeV resonance, we have estimated from formula (1) the peak cross section as seen superposed on the continuum of potential scattering. The results are shown in Table II. In the column labeled "Expt" the experimental value

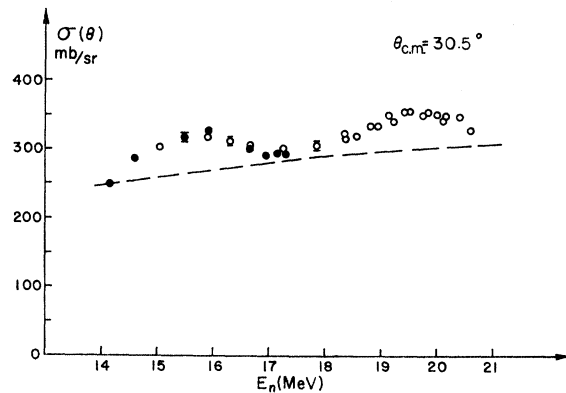


FIG. 9. Excitation curve for the differential elastic scattering at 30.5° (c.m.); the measurements were normalized at 14.2 MeV (Ref. 13). Solid and open circles correspond to measurements with deuterons of 1.5 and 3 MeV, respectively.

TABLE II. Measured and calculated peak resonance cross sections in mb for $\mu=0.7$. Figures with an asterisk are derived from resonance term and interference terms obtained from the incoherent part (B) of the potential scattering; figures in parentheses denote the depths of dips in the curve of scattering cross section against energy.

$\theta_{c.m.}$	Expt	$l=0$ $j=\frac{1}{2}$	$\frac{1}{2}$	$l=1$ $\frac{3}{2}$	$\frac{3}{2}$	$l=2$ $\frac{5}{2}$	$\frac{5}{2}$	$l=3$ $\frac{7}{2}$	$\frac{7}{2}$	$l=4$ $\frac{9}{2}$
90°	5	25	15*	(5)*	26	45	7	30	(15)	(17)
54.7°	12	28	15	30	3*	3*	30	35	70	40
39.2°	50	60	60	110	70	100	16*	35*	(70)	(55)
30°	60	100	90	180	125	200	100	170	10*	40*

of the peak cross section is given; as pointed out before this value is lower than it would be if seen with better energy resolution. Under these circumstances the peak value might be higher than given in the table. It will be seen that the angular momenta $l=2, 3,$ and 4 are definitely excluded because they would give much smaller resonance contributions than observed at the angles where $P_2, P_3,$ and $P_4,$ respectively, are zero. The peaks are roughly proportional to μ because most of the contributions are due to the interference terms. However, at these angles, the incoherent term is the main contribution to the peak, and since this depends on the spin-orbit coupling, its contribution to elastic scattering generally is least well known. If μ were raised to unity, $l=4$ would be excluded because, at 90° , it would give a dip and not a peak; and $l=3$ would be excluded as giving too great a peak at 55° . There remains only $l=0$ or $l=1$. Of these the former could give agreement only by reducing μ to about 0.4, which is unacceptable because no resonance was seen in the inelastic scattering. For $l=1$, the most probable choice is $j=\frac{1}{2}$, for the effect expected of $j=\frac{3}{2}$ is very small, and likely to produce a dip rather than a peak.

These conclusions are confirmed by a comparison between the observed total elastic cross section and that

calculated by integration of Eq. (1), which gives

$$\int \mu^2 \lambda^2 [P_l^2(\cos\theta) + g_{\pm}^2 P_l^2(\cos\theta)] \sin^2\phi d\Omega \\ + 2\mu\lambda g_{\pm} \int A(\theta) P_l(\cos\theta) \sin\phi \cos(\phi - \delta_A) d\Omega,$$

neglecting the term containing B . The first term of this equation is the usual resonance term $4\pi\mu^2\lambda^2 g_{\pm}^2 \sin^2\phi$. The net result depends about equally on the resonance and the interference term. For $\mu=0.7$, the results for $l=0$ and 1 are shown in Table III. The case $j=\frac{3}{2}$ seems to be definitely ruled out. No higher angular momenta are included for they give peak heights that would require far too low a value of μ to give agreement with experiment.

These calculations, as mentioned above, have been carried out only at 16 MeV. Since the amplitude and phases of the potential scattering do not change very rapidly with energy, the general conclusions arrived at for the 15.8-MeV resonance also apply to the broader level near 19 MeV. Both resonances therefore seem to be $j=\frac{1}{2}$. The sum of the ratios of the reduced widths divided by the Wigner limit is about 0.5.

ACKNOWLEDGMENTS

The authors wish to acknowledge the assistance of A. Rego and V. Mistry in making some of these measurements; valuable discussions with Dr. W. R. Coker and Dr. T. Griffy on theoretical aspects; and advice from Dr. G. Marcazzan concerning construction of the neutron recoil spectrometer.

TABLE III. Total elastic scattering cross sections in mb for the 15.8-MeV resonance.

Experimental (from Fig. 5)	Calculated ($\mu=0.7$)		
	$l=0, j=\frac{1}{2}$	$l=1, j=\frac{1}{2}$	$l=1, j=\frac{3}{2}$
≥ 170	190	250	500